

Solar Energy Transfer Through Semitransparent Plate Systems

Steven J. Mitts* and Theodore F. Smith†
The University of Iowa, Iowa City, Iowa

The objective of this study is to develop a model to examine the interaction of solar radiation with systems consisting of semi-transparent plates. The embedding technique is developed so that the model considers both beam and diffuse solar energy entering a system, as well as the conversion of beam to diffuse energy that may occur in some plates. The fraction of the incident radiant energy absorbed by each plate is determined as well as the energy reflected and transmitted by the system. Results are presented to illustrate the absorptances for systems composed of such devices as glass panes and slat-type shades.

Nomenclature

a	= apparent solar absorptance
A^b, A^{bd}, A^d	= beam, beam-diffuse, and diffuse top-of-the-stack absorptance
$\bar{A}_{N,i}$	= within-stack absorptance of plate i of N plates
\bar{A}^b	= beam within-stack absorptance
C	= slat spacing, m
I_b, I_d	= beam and diffuse components of solar energy, W/m^2
I	= irradiation, W/m^2
J	= radiosity, W/m^2
N	= number of plates
q_a	= within-stack absorbed energy, W/m^2
r	= apparent solar reflectance
R^b, R^{bd}, R^d	= beam, beam-diffuse, and diffuse stack reflectance
\bar{R}^b	= beam stack reflectance
t	= apparent solar transmittance
T^b, T^{bd}, T^d	= beam, beam-diffuse, and diffuse top-of-the-stack transmittance
W	= slat width, m
α^*	= slat solar absorptance
ϕ_b	= solar beam angle, deg
ψ	= slat angle, deg
Subscripts	
b, d	= beam and diffuse
bb, bd, dd	= beam-beam, beam-diffuse, and diffuse-diffuse
Superscripts	
$'$	= apparent property for energy incident on plate bottom
b, d	= beam and diffuse

Introduction

THE rising cost of building heating and cooling has increased the interest in the development of more energy-efficient building components, such as solar collector and window systems. These systems typically consist of plates with low insulating values that allow significant amounts of thermal energy to escape.

One method of increasing the insulating value of these systems is to use multiple layers, such as several plates of glass separated by a nearly stagnant airspace. To help control the radiative heat transfer through the system, the plates may be given special radiative properties by attaching films with antireflection coatings, using low-emittance coatings or grinding the surface so that the solar energy is transmitted and reflected as diffuse energy. Another method, as studied by Smith and Mitts,¹ uses opaque slats to control the solar energy and thermal radiative transfer through these systems. The use of devices such as honeycombs or slats to reduce the heat loss by convection between the plates has been proposed.² The convection suppression devices are highly transparent layers that allow passage of solar energy and may affect the thermal radiative heat transfer through the system. To examine the performance of these systems, it is necessary to determine the solar absorption of each plate as well as the energy reflected and transmitted by the system.

When a system is partially transparent to radiation, the radiative transfer through the system is important, particularly when the system is exposed to a high-temperature source such as the sun. Edwards³ presented the embedding method as a means of calculating the absorption in each plate in a stack of semitransparent plates over an opaque absorber. The method is convenient to execute and is conducive to studying the effects that changes of plate properties and locations have on the system. Because of the desire to model systems that include shades, the method needs to be extended to account for the transition of beam energy, as associated with the beam component of solar energy, to a diffuse energy component.

The objective of this study is to develop a model to examine the interaction of solar radiation with systems consisting of semitransparent plates. The embedding technique is developed so that it can model both beam and diffuse solar energy entering a system, as well as the change from beam to diffuse energy that may occur in some plates. The fraction of the incident radiant energy absorbed by each plate is determined, as well as the energy reflected back out of the system.

Embedding Technique

The embedding technique is developed based on the system depicted in Fig. 1. This system consists of N plates, which together make up the system stack. The plates are parallel and infinite in length and depth. The media between the plates are assumed to be radiatively transparent with a refractive index of unity. Solar energy incident on the top of the stack may have both beam and diffuse components of I_b and I_d , respectively. At the top of each plate, the inward-directed radiant fluxes are labeled I_i for the irradiation, and the outward-directed fluxes are labeled J_i for the radiosity of each plate. Each flux has both beam and diffuse components.

Presented as Paper 86-1293 at the AIAA/ASME 4th Thermophysics and Heat Transfer Conference, Boston, MA, June 2-4, 1986; received April 11, 1986; revision submitted Sept. 18, 1986. Copyright © American Institute of Aeronautics and Astronautics, Inc., 1987. All rights reserved.

†Professor, Department of Mechanical Engineering. Member AIAA.

Plate 1 is an opaque absorber, which provides a convenient reference from which the embedding analysis can be started. A solar collector generally includes an absorber plate as a physical element of the system. When modeling a window system, the room acts as the absorber, absorbing some of the energy transmitted through the system and reflecting the remainder back out the window. The remaining plates are semitransparent. A plate has eight apparent radiative properties for radiant energy incident on either side of the plate. The apparent properties^{1,4} are based on the surface properties and assume that the reflections that occur at an interface between different media are either specular or diffuse. There are three possible transmittances, t_{bb} , t_{bd} , and t_{dd} ; three possible reflectances, r_{bb} , r_{bd} , and r_{dd} ; and two absorptances, a_b and a_d . The lowercase letters of a , r , and t denote apparent or overall radiative properties of a plate. Subscripts b and d denote, respectively, beam and diffuse energy. For the double-subscripted properties, the first subscript indicates the form of energy that is incident on the plate, and the second subscript refers to the form the energy has when it leaves the plate. As an example, r_{bd} is the quantity of a beam energy that is incident on a plate and reflected back as diffuse energy. For absorptances, only a single subscript denoting the form of the incident energy is used. A prime superscript is used to designate the properties for energy incident on the bottom surface. For diffuse energy, the transmittances for the top and bottom surfaces are equal, i.e., $t_{dd} = t'_{dd}$. Therefore, each plate has 15 radiative properties that satisfy energy conservation statements for both beam and diffuse components.

The embedding technique begins from the absorber, increasing the size of the stack one plate at a time. As each plate is added, the embedding properties of stack reflectance, top-of-the-stack transmittance, and top-of-the-stack absorptance are calculated. The beam stack reflectance R^b , where upper-case letters refer to stack radiative properties, is the fraction of beam solar energy incident on the stack that is reflected, taking into account all the specular reflections that occur throughout the stack. Similarly, R^d is the diffuse stack reflectance, and R^{bd} is the stack reflectance of beam energy that is converted to diffuse. Top-of-the-stack transmittances T^b , T^d , and T^{bd} are the transmittances through the i th layer, taking into account the multiple interactions of the radiant energy with each layer. Similarly, top-of-the-stack absorptances A^b , A^d , and A^{bd} are also calculated. All plate and stack properties are calculated for a single wavelength, angle of incidence, and component of polarization of the beam and diffuse solar energy where the directional dependence for diffuse properties is not required. These dependencies are understood unless otherwise noted.

Consider the i th plate in the stack of Fig. 1, and assume that the $i+1$ to N plates have not been added to the stack. The plate has irradiations of I_i^b and I_i^d that are equal to the beam and diffuse components of solar energy when the plate is on the top of the stack, as it is now. Assume that R_{i-1}^b , R_{i-1}^{bd} , and R_{i-1}^d have already been calculated. Concentrating on the exchange of energy beneath plate i and the equations due to beam energy only, the radiosity is

$$J_{i-1}^b = I_{i-1}^b R_{i-1}^b \quad (1)$$

where the method for using R_{i-1}^b should be noted. The irradiation on plate $i-1$ is

$$I_{i-1}^b = I_i^b t_b(i) + J_{i-1}^b r'_{bb}(i) \quad (2)$$

where the notation of (i) denotes the apparent property of plate i . A similar pair of equations for the diffuse component follows:

$$J_{i-1}^d = I_{i-1}^b R_{i-1}^{bd} + I_{i-1}^d R_{i-1}^d \quad (3)$$

$$I_{i-1}^d = I_i^b t_{bd}(i) + I_i^d t_{dd}(i) + J_{i-1}^b r'_{bd}(i) + J_{i-1}^d r'_{dd}(i) \quad (4)$$

In these expressions, any changes of beam energy into diffuse energy are accounted for by multiplying the beam energy by R_{i-1}^{bd} in Eq. (3) and t_{bd} and r'_{bd} in Eq. (4).

Equations (1-4) are solved for each of the four fluxes in terms of the irradiations, the properties of the individual plates, and the stack reflectances. Equations (1) and (2) are solved to yield

$$J_{i-1}^b = I_i^b T_i^b R_{i-1}^b \quad (5)$$

$$I_{i-1}^b = I_i^b T_i^b \quad (6)$$

where the beam component of the top-of-the-stack transmittance is defined as

$$T_i^b = t_{bb}(i) / [1 - r'_{bb}(i) R_{i-1}^b] \quad (7)$$

The top-of-the-stack transmittance for plate i is the fraction of the solar energy component that is transmitted through the plate and is incident on plate $i-1$, taking into account the interaction the energy has with each plate in the stack. Equations (3) and (4) are solved simultaneously, and Eqs. (5) and (6) are substituted to yield

$$J_{i-1}^d = I_i^b [T_i^b R_{i-1}^{bd} + t_{bd}(i) R_{i-1}^d + T_i^b R_{i-1}^b r'_{bb}(i) R_{i-1}^d] / [1 - r'_{dd}(i) R_{i-1}^d] + I_i^d T_i^d R_{i-1}^d \quad (8)$$

$$I_{i-1}^d = I_i^b [t_{bd}(i) + T_i^b R_{i-1}^b r'_{bd}(i)] + T_i^b R_{i-1}^{bd} r'_{dd}(i) / [1 - r'_{dd}(i) R_{i-1}^d] + I_i^d T_i^d \quad (9)$$

where the diffuse component of the top-of-the-stack transmittance T_i^d is obtained from Eq. (7) with b 's replaced by d 's. The diffuse radiosity in Eq. (8) and the diffuse irradiation in Eq. (9) are both written as the sum of two components, where the first component is multiplied by the beam irradiation I_i^b and the second is multiplied by the diffuse irradiation I_i^d . Thus,

$$J_{i-1}^d = b J_{i-1}^d + d J_{i-1}^d \quad (10)$$

$$I_{i-1}^d = b I_{i-1}^d + d I_{i-1}^d \quad (11)$$

where, in both equations, the forward subscripts b and d indicate the component multiplied by beam and diffuse irradiation, respectively.

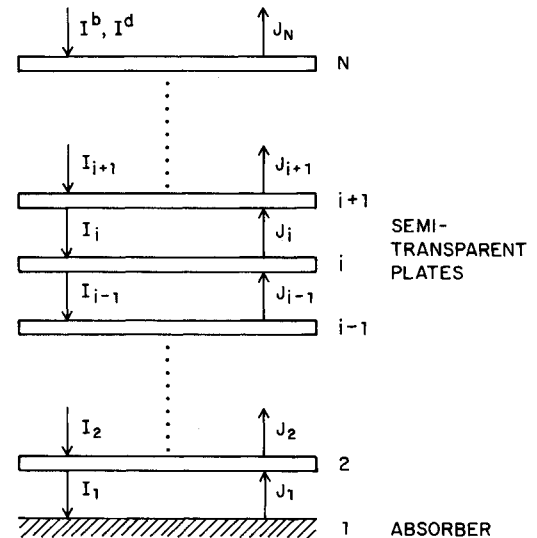


Fig. 1 Schematic diagram of embedded plates.

Expressions for the radiosities for plate i are as follows:

$$J_i^b = I_i^b r_{bb}(i) + J_{i-1}^b t'_{bb}(i) \quad (12)$$

$$J_i^d = I_i^b r_{bd}(i) + I_i^d r_{dd}(i) + J_{i-1}^b t'_{bd}(i) + J_{i-1}^d t'_{dd}(i) \quad (13)$$

When Eqs. (5) and (8) are substituted, these expressions can be rearranged to yield

$$J_i^b = I_i^b [r_{bb}(i) + T_i^b R_{i-1}^b t'_{bb}(i)] \quad (14)$$

$$J_i^d = I_i^b \{ [T_i^b R_{i-1}^{bd} + t_{bd}(i) R_{i-1}^d] + T_i^b R_{i-1}^b r'_{bd}(i) R_{i-1}^d \} t'_{dd}(i) / [1 - r'_{dd}(i) R_{i-1}^d] + r_{bd}(i) + T_i^b R_{i-1}^b t'_{bd}(i) \} + I_i^d [r_{dd}(i) + T_i^d R_{i-1}^d t'_{dd}(i)] \quad (15)$$

Similar to the diffuse expressions in Eqs. (8) and (9), the diffuse radiosity is rewritten as

$$J_i^d = {}_b J_i^d + {}_a J_i^d \quad (16)$$

The recurring properties in this analysis are the stack reflectances derived from the radiosities leaving plate i normalized by the corresponding irradiation. The expression for the beam stack reflectance is given by

$$R_i^b = J_i^b / I_i^b = r_{bb}(i) + T_i^b R_{i-1}^b t'_{bb}(i) \quad (17)$$

The diffuse stack reflectance is obtained from Eq. (17) by substituting ${}_a J_i^d$ for J_i^b and the sub- and superscripts d for the sub- and superscripts b . The beam-diffuse stack reflectance is similar to the beam-diffuse reflectance in that they both account for the conversion of beam irradiation into diffuse energy. The beam-diffuse stack reflectance is given by the ratio of the b component of the diffuse radiosity from Eq. (16) normalized by the beam irradiation as follows:

$$R_i^{bd} = {}_b J_i^d / I_i^b = r_{bd}(i) + T_i^b R_{i-1}^b t'_{bd}(i) + [T_i^b R_{i-1}^{bd} + t_{bd}(i) R_{i-1}^d] + T_i^b R_{i-1}^b r'_{bd}(i) R_{i-1}^d t'_{dd}(i) / [1 - r'_{dd}(i) R_{i-1}^d] \quad (18)$$

The top-of-the-stack transmittances for the beam and diffuse component were previously defined in terms of the plate properties. In terms of the irradiances on plates i and $i-1$, these are given as

$$T_i^b = I_{i-1}^b / I_i^b; \quad T_i^d = {}_a I_{i-1}^d / I_i^d \quad (19)$$

The beam-diffuse top-of-the-stack transmittance is similar to the beam-diffuse transmittance in that they both account for the conversion of beam irradiation into diffuse irradiation and is given by the component of diffuse irradiation on plate $i-1$, ${}_b J_{i-1}^d$, from Eq. (11) normalized by the beam solar energy.

$$\begin{aligned} T_i^{bd} &= {}_b J_{i-1}^d / I_i^b \\ &= [t_{bd}(i) + T_i^b R_{i-1}^b r'_{bd}(i) + T_i^b R_{i-1}^{bd} r'_{dd}(i)] / [1 - r'_{dd}(i) R_{i-1}^d] \end{aligned} \quad (20)$$

The top-of-the stack absorptance is the absorbed solar energy plus the absorbed radiosity from the bottom normalized by the incident solar energy. The beam component of the top-of-the-stack absorptances is expressed as

$$\begin{aligned} A_i^b &= [a_b(i) I_i^b + a'_b(i) J_{i-1}^b] / I_i^b \\ &= a_b(i) + T_i^b R_{i-1}^b a'_b(i) \end{aligned} \quad (21)$$

The diffuse component is obtained by substituting ${}_a J_{i-1}^d$ from Eq. (10) for J_{i-1}^b and the "d" sub- and superscripts for the "b" sub- and superscripts in Eq. (21). The beam-diffuse top-of-the-stack absorptance is the absorbed beam-diffuse radiosity from Eq. (10) normalized by the beam solar energy and is given by

$$\begin{aligned} A_i^{bd} &= a'_d(i) {}_b J_{i-1}^d / I_i^b = [T_i^b R_{i-1}^{bd} + t_{bd}(i) R_{i-1}^d] \\ &+ T_i^b R_{i-1}^b r'_{bd}(i) R_{i-1}^d a'_d(i) / [1 - r'_{dd}(i) R_{i-1}^d] \end{aligned} \quad (22)$$

Because radiant energy is absorbed only on the bottom surface for the beam-diffuse component, it has a value of zero for plate 1 since this plate is opaque.

Once all of the stack properties have been calculated, the three components of the within-stack absorptance are calculated for each plate. The within-stack absorptance $\bar{A}_{N,i}$ is the fraction of incident solar energy absorbed by the i th plate in a stack of N plates. For the top plate in the stack, the within-stack absorptance is simply the top-of-the-stack absorptance. Below the top plate, the energy available to be absorbed is reduced because not all of the solar energy incident on the system is transmitted through each plate. To determine the within-stack absorptance in these plates, the irradiation on plate i is determined by multiplying the solar energy component by the top-of-the-stack transmittances of plates N to $i+1$. This reduced irradiation is multiplied by the top-of-the-stack absorptance of plate i to obtain the within-stack absorptance for the beam component as follows:

$$\bar{A}_{N,i}^b = A_i^b \prod_{j=i+1}^N T_j^b \quad (23)$$

The beam-diffuse within-stack absorptance is obtained by substituting the superscript bd for the superscript b on the A and A terms in Eq. (23). The beam top-of-the-stack transmittance is used in the expression for the beam-diffuse within-stack absorptance, even though this expression accounts for the absorption of diffuse energy. This is because the energy is not converted to diffuse energy until it strikes plate $i-1$ and leaves as radiosity ${}_b J_{i-1}^d$, therefore, the energy must be transmitted through plate i as beam energy. The beam energy is converted to diffuse energy in the beam-diffuse within-stack absorptance by the beam-diffuse top-of-the-stack absorptance term.

It is instructive to illustrate the diffuse within-stack absorptance by first introducing the diffuse within-stack absorbed energy as follows:

$$\begin{aligned} q_{a,i}^d &= A_i^d \sum_{j=i+1}^N \left[\left(\prod_{k=i+1}^{j-1} T_k^d \right) T_j^{bd} \left(\prod_{l=j+1}^N T_l^b \right) \right] I_i^b \\ &+ A_i^d \left(\prod_{k=i+1}^N T_k^d \right) I_i^d \end{aligned} \quad (24)$$

The first component accounts for the beam solar energy that is absorbed by plate i after being transmitted as beam energy down to plate $j+1$, converted to diffuse energy at plate j , and transmitted as diffuse energy from plate $j-1$ to plate $i+1$. The second component accounts for the diffuse solar energy incident on the system that is transmitted diffusely to plate i and absorbed. In the first component of Eq. (24), there are two special cases to consider. When $j=i+1$, there is no T_k^d term, which means that the beam energy is converted to diffuse energy at plate $i+1$ directly above the i th plate. Similarly, when $j=N$, there is no T_j^b term, meaning that the beam energy is converted to diffuse energy at the top plate of the stack. Under either of these conditions, the respective multiplication products, $\prod T_k^d$ or $\prod T_j^b$, are set equal to unity. Equation (24) is

described as the sum of the beam-diffuse within-stack absorbed energy and the diffuse-diffuse within-stack absorbed energy and is written as

$$q_{a,i}^d = b q_{a,i}^d + d q_{a,i}^d \quad (25)$$

The diffuse within-stack absorptance is the sum of the two components; the first component is $b q_{a,i}^d$ normalized by I_b , and the second component is $d q_{a,i}^d$ normalized by I_d . Thus,

$$\bar{A}_{N,i}^d = b \bar{A}_{N,i}^d + d \bar{A}_{N,i}^d \quad (26)$$

Conservation of energy for the stack requires that the sum of the absorbed energy within each plate and energy leaving the top plate is equal to the solar energy incident upon the system. Therefore, the conservation of energy for the beam solar energy is

$$\sum_{i=1}^N (\bar{A}_{N,i}^b + b \bar{A}_{N,i}^d + \bar{A}_{N,i}^{bd}) + (R_N^b + R_N^{bd}) = 1 \quad (27a)$$

and the corresponding equation for the diffuse component of solar energy is

$$\sum_{i=1}^N d \bar{A}_{N,i}^d + R_N^d = 1 \quad (27b)$$

Equation (27) then provides a check regarding the accuracy of the results from the embedding analysis.

Results and Discussion

The transfer of beam energy through a double glass plate system with a shade demonstrates the capabilities of the embedding technique because beam solar energy is converted to diffuse energy when it interacts with the shade. Results for the transfer of beam solar energy through a window system consisting of three combinations of two glass panes and a shade system are examined. The window system is modeled on top of a diffusely reflecting absorber plate, representing the room interior, that has beam and diffuse absorptances of 0.9. The specularly reflecting glass plates have indices of refraction of 1.5, absorption coefficients of 0.299 cm^{-1} , and thicknesses of 0.317 cm. The glass and shade properties were determined using the methods described elsewhere,^{1,4} where, for the shade, a slat width to spacing ratio (W/C) of 1.2 is used.

Results are presented for the window system components in three combinations, namely shade-glass-glass (SGG), glass-shade-glass (GSG), and glass-glass-shade (GGS). The first component is the inside of the window, farthest away from the solar energy source, and the last component is the exterior component, nearest the incident solar energy. Stack reflectance \bar{R}^b and within-stack absorptance \bar{A}_i^b are the sums of the respective components due to beam solar energy, i.e., $\bar{R}^b = R^b + R^{bd}$ and $\bar{A}_i^b = \bar{A}_i^b + \bar{A}_i^{bd} + b \bar{A}_i^d$. These values are plotted vs beam angle ϕ_b . The stack reflectance and within-stack absorptances, due to diffuse solar energy are independent of beam angle. The results for beam and diffuse solar energy are dependent on the apparent radiative properties of the shade system, particularly at near-normal angles of incidence where the glass plates are highly transparent. In some positions of the shade slat angle and solar beam position, a

partial beam component that is not the same width as the incident beam is transmitted by the shade system. When a glass plate is behind the shade, this partial beam experiences specular reflection from the glass plate, and the specularly reflected partial beam then interacts with the shade. The shade model¹ allows for full beams only. Thus, to account for the energy content of the partial beam, the partial beam is treated as a full beam. This is plausible in view of the low reflectance for near-normal incidence for the glass plate. When larger incident beam angles are encountered, the partial beam is generally zero as a result of the shade beam-beam transmittance being zero.

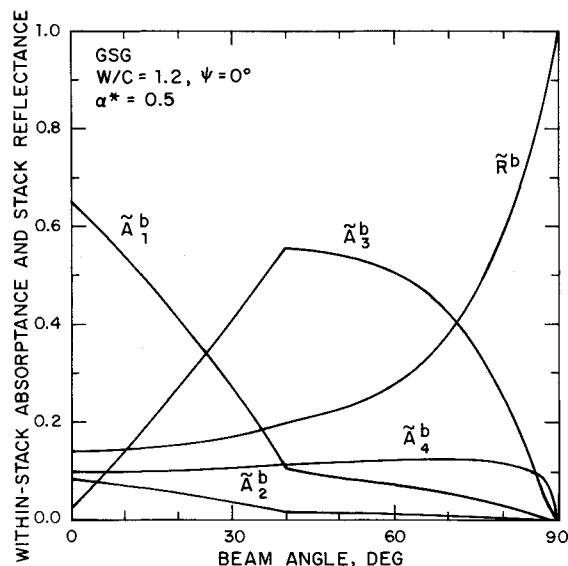


Fig. 2 Embedding properties of a GSG window system.

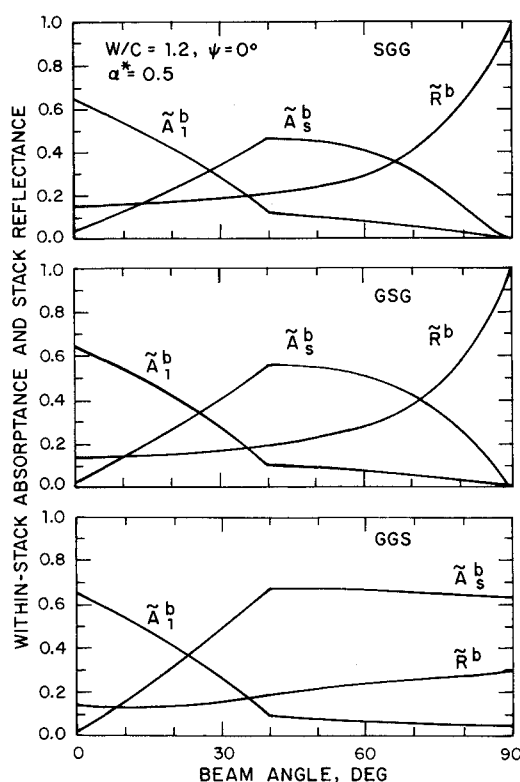


Fig. 3 Effect of shade location in a three-plate window system.

Table 1 Diffuse stack properties

Configuration	Ψ , deg	\bar{R}^d	$d \bar{A}_1^d$	$d \bar{A}_s^d$
SGG	0	0.2314	0.2603	0.3539
GSG	0	0.2630	0.2616	0.2685
GGS	0	0.1729	0.2637	0.4662
GSG	60	0.3219	0.1281	0.4044

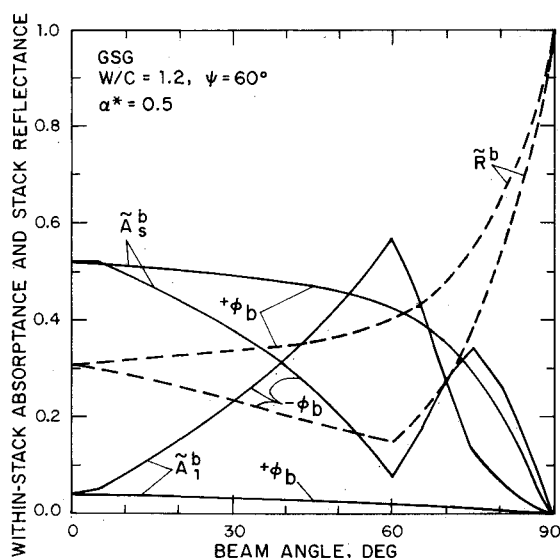


Fig. 4 Effect of slat angle on stack properties.

Results are shown for a window system where the shade has slat solar absorptances of $\alpha_b^* = \alpha_d^* = 0.5$ and a slat angle of $\Psi = 0$ deg corresponding to the fully opened position. The GSG configuration was chosen to show the trends of the within-stack absorbance of each system component and the stack reflectance. Results shown in Fig. 2 are applicable to either positive or negative beam angles. A beam angle of zero implies that the beam component is normal to the window system. The energy absorbed by the room interior is plotted as the within-stack absorbance of plate 1, \bar{A}_1^b and the energy absorbed by each plate is labeled \bar{A}_2^b , \bar{A}_3^b , and \bar{A}_4^b . In this case, \bar{A}_3^b is for the shade and \bar{A}_2^b and \bar{A}_4^b are for the interior and exterior glass plates, respectively. At normal incidence, the beam-beam transmittance of the shade is unity, and maximum energy is transmitted to the room interior, resulting in a large value for \bar{A}_1^b . The within-stack absorbance of the shade is not zero due to the energy diffusely reflected from plate 1. For angles of incidence less than 40 deg, the stack properties are governed by the apparent properties of the shade. At these angles, the beam-beam transmittance of the shade is decreasing, whereas the apparent absorbance of the shade increases, resulting in less energy transmitted to the room interior and absorbed by plate 1. The discontinuity in the curves at $\phi_b = 40$ deg is where the shade beam-beam transmittance goes to zero and the shade properties become slightly less responsive to changes in the beam angle. As the beam angle increases past 60 deg, the reflectance of the exterior glass plate increases, causing the stack reflectance to increase and the within-stack absorbances to decrease. The within-stack absorbances of the two glass plates are also shown in Fig. 2. They are relatively small and do not vary greatly as a function of beam angle. Since they are typical of the other glass plate within-stack absorbances, they are not included in subsequent plots.

The influence of the location of the shade in the window system is shown in Fig. 3, where the shade used to produce the results of Fig. 2 has been examined in each of the three locations. The stack reflectance and the within-stack absorbances of the room interior and of the shade are plotted as a function of beam angle. Because the location of the shade is not the same in each plot, the shade within-stack absorbance is labeled as \bar{A}_s^b , where the subscript s denotes the shade. Comparison of the results from the three configurations shows that for all beam angles, the within-stack absorbances of the room interiors are, with a single exception, nearly identical. This indicates that, for this shade configuration, regardless of the order of these components, the fraction of incident energy absorbed by the room interior remains nearly constant. The ex-

ception is in the GGS configuration, where \bar{A}_s^b does not go to zero at $\phi_b = 90$ deg, as do the \bar{A}_s^b curves for the GSG and SGG configurations. In the latter two configurations, the stack reflectance goes to unity at $\phi_b = 90$ deg because a glass plate is positioned on the exterior, and its reflectance goes to unity at this angle. In contrast, the GGS configuration has the shade on the exterior, which allows some beam-diffuse transmittance, thereby providing energy to be absorbed by interior plates even at large angles of incidence.

The within-stack absorbances of the shade are not the same in the different configurations. At $\phi_b = 0$ deg, the shade within-stack absorbance is approximately 0.04 for all three configurations, but for $0 < \phi_b < 40$ deg, each \bar{A}_s^b increases to a different maximum at $\phi_b = 40$ deg, where $\bar{A}_s^b = 0.67$, 0.56, and 0.46, respectively, for the GGS, GSG, and SGG cases. Hence, the shade absorbs less energy as the number of glass plates between the shade and beam source increases. For the two configurations in which the stack reflectances go to unity at $\phi_b = 90$ deg, the shade within-stack absorbance goes to zero. In the GGS configuration, \bar{A}_s^b remains nearly constant for $40 < \phi_b < 90$ deg, and the shape of the \bar{A}_s^b plot is similar to that of the shade beam absorptance.¹

An example of the embedding results for a window system with a slat angle not equal to zero is shown in Fig. 4. The same GSG configuration in Fig. 2 is used, but $\Psi = 60$ deg. At $\phi_b = -60$ deg, the solar beam component is parallel to the slats. These results are not symmetric about $\phi_b = 0$ deg, therefore, results are plotted for positive and negative beam angles. Consider first the results for $\phi_b > 0$ deg. For all positive beam angles, the apparent shade property of beam-beam transmittance is zero and there are no discontinuities in the embedding curves. Comparison of the results to Fig. 2 shows that the stack reflectance is consistently larger for $\Psi = 60$ deg, and the absorber within-stack absorbance is consistently smaller. These trends can be attributed to the smaller apparent transmittance and larger apparent absorbance of the shade at $\Psi = 60$ deg. The within-stack absorbance of the shade is maximum at $\phi_b = 0$ deg, where maximum slat surface area is exposed to beam solar energy. As ϕ_b is increased, the slat area exposed is decreased, as well as \bar{A}_s^b . When the beam angle goes above 60 deg, \bar{A}_s^b decreases more rapidly, due to the increase in stack reflectance caused by the reflectance of the exterior glass plate.

When $\phi_b < 0$ deg, discontinuities exist in the curves of the embedding properties. At $\phi_b = -60$ deg, \bar{A}_1^b reaches a maximum and \bar{A}_2^b is at a minimum. These limits occur when the beam-beam transmittance of the shade is unity. Similar limits occurred when $\Psi = 0$ deg at $\phi_b = 0$ deg, but the limits for the $\Psi = 60$ -deg case are less extreme, due to the increased reflection from the glass plates. For $\phi_b < -60$, \bar{A}_s^b begins to increase as the shade beam-beam transmittance decreases, however, at $\phi_b = -75$ deg, the shade within-stack absorbance begins to decrease again when the stack reflectance begins to approach unity at $\phi_b = -90$ deg. If the slat angle is -60 deg, the results in Fig. 4 would still be applicable, but the curves for the positive and negative beam angles would be interchanged. For a system with slats at other angles, the results are similar to those displayed in Fig. 4. At $\Psi = 90$ deg, \bar{A}_1^b is zero and \bar{A}_s^b and \bar{R}^b are nearly constant for $0 < \phi_b < 45$, acquiring values near the slat solar absorptance and reflectance, respectively. At large beam angles, the reflectance of the glass begins to dominate and the stack reflectance goes to unity, and \bar{A}_s^b goes to zero as ϕ_b goes to 90 deg. In general, the window system results show that for beam angles less than 60 deg, the solar energy reflected, absorbed, and transmitted by such a system is highly dependent on the apparent properties of the shade. As the beam angle approaches 90 deg, the energy transfer is dominated by the plate on the exterior of the configuration.

The results for diffuse solar energy are shown in Table 1 for the three window configurations. Moving the shade net to the absorber yields maximum stack reflectance and minimum shade within-stack absorbance. When the shade is on the ex-

terior, nearest to the solar energy source, the stack reflectance is small and the shade within-stack absorptance is large. For all three shade locations, the absorber within-stack absorptances are nearly identical, the difference caused by energy reflected by the absorber and rereflected back to the absorber in different magnitudes. When the slat solar absorptances are varied, the shade within-stack absorptance increases when the apparent absorptance increases and the stack reflectance and absorber within-stack absorptance decrease. The opposite occurs when the apparent absorptance of the shade is decreased. As discussed earlier, increasing the shade angle increases the apparent absorptance and reflectance, and decreases the apparent transmittance. This results in the large values of shade within-stack absorptance and stack reflectance and small absorber within-stack absorptance. The results for diffuse solar energy show that the embedding results are also dependent on the apparent properties of the shade.

Conclusions

A model has been developed to study the transfer of solar energy through systems consisting of semitransparent parallel plates. The embedding technique was extended to model both beam and diffuse components of solar energy, as well as to account for the possible change from beam energy to diffuse energy. The embedding method yields the within-stack absorptance that gives the fraction of incident solar energy absorbed by each plate and the stack reflectance. The stack

transmittance is determined by calculating the energy absorbed by a black absorber plate. The embedding results indicate that the arrangement of nonidentical plates can affect the quantities of solar energy absorbed, reflected, and transmitted by the system. Further embedding results for specific window systems with shades show a dependence on the shade apparent properties at low beam angles and on the properties of the exterior plate at large beam angles. The embedding technique provides a convenient method for modeling the transfer of solar energy in systems such as windows and flat-plate solar collectors and is conducive to comparing numerous permutations of a system or several unique systems.

References

- ¹Smith, T. F. and Mitts, S. J., "Radiative Properties of Shade Systems," *Alternative Energy in the Midwest Conference Proceedings*, Vol. 1, 1985, pp. 2.21-32.
- ²Symons, J. G., "Calculation of the Transmittance-Absorptance Product for Flat-Plate Collectors with Convection Suppression Devices," *Solar Energy*, Vol. 33, 1984, pp. 637-640.
- ³Edwards, D. K., "Solar Absorption by Each Element in an Absorber-Coverglass Array," *Solar Energy*, Vol. 19, 1977, pp. 401-402.
- ⁴Siegel, R. and Howell, J. R., *Thermal Radiation Heat Transfer*, 2nd ed., McGraw-Hill, New York, 1981.

From the AIAA Progress in Astronautics and Aeronautics Series...

FUNDAMENTALS OF SOLID-PROPELLANT COMBUSTION - v. 90

*Edited by Kenneth K. Kuo, The Pennsylvania State University
and*

Martin Summerfield, Princeton Combustion Research Laboratories, Inc.

In this volume distinguished researchers treat the diverse technical disciplines of solid-propellant combustion in fifteen chapters. Each chapter presents a survey of previous work, detailed theoretical formulations and experimental methods, and experimental and theoretical results, and then interprets technological gaps and research directions. The chapters cover rocket propellants and combustion characteristics; chemistry ignition and combustion of ammonium perchlorate-based propellants; thermal behavior of RDX and HMX; chemistry of nitrate ester and nitramine propellants; solid-propellant ignition theories and experiments; flame spreading and overall ignition transient; steady-state burning of homogeneous propellants and steady-state burning of composite propellants under zero cross-flow situations; experimental observations of combustion instability; theoretical analysis of combustion instability and smokeless propellants.

For years to come, this authoritative and compendious work will be an indispensable tool for combustion scientists, chemists, and chemical engineers concerned with modern propellants, as well as for applied physicists. Its thorough coverage provides necessary background for advanced students.

Published in 1984, 891 pp., 6 × 9 illus. (some color plates), \$60 Mem., \$85 List; ISBN 0-915928-84-1

TO ORDER WRITE: Publications Dept., AIAA, 370 L'Enfant Promenade S.W., Washington, D.C. 20024-2518